

AD-A067 114

HONEYWELL INC MINNEAPOLIS MINN SYSTEMS AND RESEARCH DIV
SPECTRAL REPRESENTATION OF TRANSIENT WAVEFORMS, (U)
1966 C R ARNOLD
66-38

F/G 20/1

UNCLASSIFIED

NL

OF |
AD
A067114



END
DATE
FILMED
6 --79
DDC

LEVEL II

MOST PROJECT - 3

Document No. 66-38

①

9703

SPECTRAL REPRESENTATION OF TRANSIENT WAVEFORMS

by

Charles R. Arnold

Good.

ADA067114

DDC FILE COPY

Presented at the
SPECTRUM ANALYSIS TECHNIQUES SYMPOSIUM
Honeywell Research Center
September 20 and 21, 1966

DDC
RECEIVED
APR 9 1979
F

DISTRIBUTION STATEMENT A

Approved for public release;
Distribution Unlimited

HONEYWELL Systems & Research Division

Handwritten initials/signature

6

SPECTRAL REPRESENTATION OF TRANSIENT WAVEFORMS.

by

10 Charles R. Arnold

12 37 p.

11 2966

14 66-38

Presented at the
SPECTRUM ANALYSIS TECHNIQUES SYMPOSIUM
Honeywell Research Center
September 20 and 21, 1966

170 184

DDC
RECEIVED
APR 9 1979
F

HONEYWELL Systems & Research Division

Printed in U.S.A.

170 184

66-38

set

SPECTRAL REPRESENTATION OF TRANSIENT WAVEFORMS

by

Charles R. Arnold
Honeywell Radiation Center

ABSTRACT

For steady-state waveform analysis, the classical (possibly smoothed) periodogram of the sampled waveform gives one an adequate spectral representation. For transient waveforms of unknown duration in noise, however, the periodogram generally fails in that it is tied to a fixed time interval. As an alternative, a digital computer program has been developed which will do time-varying spectral estimation.

Briefly, the program may be described as a digital equivalent of a constant Q comb filter bank wherein one can vary the frequency range covered and the frequency resolution (i. e. the Q). For a given specified frequency range, as one increases the frequency resolution, the program automatically selects more filters and spaces them so as to cover the specified frequency range; the various contiguous filters being overlapped at the -3 dB points. The instantaneous energy contained in each filter is used to modulate the z-axis of a CRT display and hence provide a time-frequency-intensity plot of the time varying spectrum.

Results obtained from the computer program upon real data are given.

SEARCHED BY	
WFO	Write Section <input checked="" type="checkbox"/>
DDG	Buff Section <input type="checkbox"/>
UNANNOUNCED	<input type="checkbox"/>
JUSTIFICATION	<i>for letter on file</i>
BY	
DISTRIBUTION/AVAILABILITY CODES	
Dist.	AVAIL. and/or SPECIAL
A	

I. INTRODUCTION

Consider the following problem: Given sample functions of various transient waveforms embedded in noise, how may one determine whether there is any natural grouping of the transients into classes causally related to the mechanism which generated the transients. From past work in steady-state system evaluation, one knows that often the power spectrum of the data is a much more consistent basis for classification than the raw noise corrupted waveform. Thus, one is motivated to determine a spectral representation (or signature) of the transients. As to practical realization of the above problem, one may think in terms of:

1. The classification of passing vehicular traffic in a noisy acoustic background
2. The classification of both man-made and biologically generated transients in an ocean background
3. The discrimination between seismic events (earthquake/blast) in a noisy background

Although motivated by these classification problems, this paper is addressed only to the problem of obtaining a spectra representative of the transient waveforms. Additional details on the classification problem may be found in the accompanying paper by Swanlund.¹

If the transient waveforms presented for classification are well above the noise to the extent that their epoch and duration are easily determined, then any of the methods summarized in the recent paper "Burst Measurements in the Frequency Domain" by Cochran et al², may be used to generate a spectral pattern. However, the transient waveforms are

usually so far down into the noise that their initial epoch and duration are not readily discernible. Moreover, one is often faced with multipath problems and multiple arrivals of the transient.

To illustrate these problems, consider an example from the seismic area. Figure 1 presents a record of approximately four minutes of the output of a single seismometer. To a trained eye, the trace does contain a seismic event which happens to be a moderately strong earthquake. The initial epoch of this seismic transient is only approximately discernible and its duration is obscured by multiple arrivals. There are many other seismic events of interest which are even much further down into the noise and even their occurrence is not discernible from a single trace.



Figure 1 SEISMOGRAM CONTAINING EARTHQUAKE EVENT

All of the methods of Cochran et al,² as presented fail when the transient's epoch and duration are not known. With the duration of the transient unknown, one may conceivably choose some upper bound T_{max} as the duration of any transient of interest and then segment one's data into intervals of length T_{max} and apply any one of the techniques of reference 2 to each data segment.

This is not satisfactory, in that this arbitrary segmentation of the data may cut some occurrences in half and thus distort and/or lose the true spectral pattern. Next, one may apply the methods of reference 2 to overlapping time intervals of the data but this leads to excessive equipment requirements in the case of analogue signals and excessive computational requirements in the case of sampled data.

As an alternative, this paper presents a technique which has been implemented upon a digital computer and which provides a time-varying spectral estimate. Briefly, the program may be described as a digital equivalent of a constant Q comb filter bank wherein one can vary the frequency range covered and the frequency resolution (i. e., the Q). This program has been found to be most effective against transients in that it is not tied to a fixed interval or initial epoch. Moreover, from results to be developed below, the program does not require the detectors and integrators (low-pass filters) usually associated with filter banks (cf. Figure 2 of Reference 2) and hence does not require the additional response time which degrades transient analysis. A complete description of the program is, however, postponed until after the algorithm it uses has been motivated and mathematically justified. This is not because of the complexity of the algorithm but just the opposite, in that its simplicity is best appreciated only after having gone through its motivation.

Thus, in the next section begins a sequence of definitions, results, and related discussions most of which are well known and well worn. Some are hopefully new, but if not, their collection here may be justified in that they represent the path down which this author's thinking has evolved. The end result being the computer program which has been found to be a very effective tool in many areas of application.

II. THE PERIODOGRAM

Given a sample of continuous time data $X(t)$ of duration T , the classical Schuster periodogram (or sample spectral density function) is defined by

$$I_T(\omega) = \frac{1}{T} \left| \int_0^T X(t) e^{j\omega t} dt \right|^2 \quad (2.1)$$

Similarly, for sampled data where the sample consists of N values X_n equally spaced in time, one uses

$$I_N(\omega) = \frac{1}{N} \left| \sum_{n=1}^N X_n e^{j\omega n} \right|^2 \quad (2.2)$$

In either case, if one chooses a discrete set of frequencies, say

$$\omega_k = \frac{2\pi k}{T} \quad \text{or} \quad \omega_k = \frac{2\pi k}{N} \quad (2.3)$$

and expands the complex exponential, one finds, for example, that

$$I_T(\omega_k) = \frac{1}{T} \left\{ \left| \int_0^T X(t) \cos\left(\frac{2\pi kt}{T}\right) dt \right|^2 + \left| \int_0^T X(t) \sin\left(\frac{2\pi kt}{T}\right) dt \right|^2 \right\} \quad (2.4)$$

from which one can recognize that

$$I_T(\omega_k) = T (a_k^2 + b_k^2) \quad (2.5)$$

where the a_k and b_k are the usual Fourier coefficients. Thus it is quite natural to expect that when the data consists of a truly periodic signal well above the noise, as is often the case for steady-state phenomena, the periodogram provides a completely effective analytical tool.

When one is interested in $X(t)$ as a stochastic process, one naturally turns to consideration of the sample auto-covariance function as a vehicle for spectral estimation since theoretically the spectral density $P(\omega)$ is nothing more than the cosine transform of the auto-correlation function of the process. Specifically for discrete-time data, one introduces the sample auto-covariance sequence,

$$C_\nu = \frac{1}{N} \sum_{n=1}^{N-\nu} X_n X_{n+\nu} \quad (2.6)$$

from which it follows that

$$I_N(\omega_k) = C_0 + 2 \sum_{n=1}^{N-1} C_n \cos(n\omega_k) \quad (2.7)$$

The validity of (2.7) is a direct consequence of algebraic identities and is independent of any assumptions about the nature of the process X . This fact is often lost by some people to the extent that they will produce two different computer programs. The first program employing the direct approach (2.2) to be used on deterministic data and a second program using

(2.6) and (2.7) to be used upon random or noisy data. The truth of the matter is, given N data samples X_n , both programs (at best) can give N independent values of the sample spectral density $I_N(\omega_k)$ and these estimated values will be the same outside of minor variations introduced by different rounding errors in the two programs.

However, as is well known, when one desires a random process as the underlying model, the periodogram has its problems. It is true that the periodogram is an asymptotically unbiased estimate of the true spectral density function $P(\omega)$, i. e. ,

$$\lim_{T \rightarrow \infty} E \left\{ I_T(\omega) \right\} \rightarrow P(\omega). \quad (2.8)$$

The difficulty with the periodogram is that when used against a random process, it is not a consistent estimator in that

$$\lim_{T \rightarrow \infty} \text{Var} \left\{ I_T(\omega) \right\} \rightarrow P^2(\omega). \quad (2.9)$$

This lack of consistency is reflected in the high degree of variability between the spectral estimates from successive samples of the same noise process.

III. THE SMOOTHED PERIODOGRAM

In 1946, Daniell³ suggested how the periodogram could be made into a consistent estimator of the spectral density. His solution was in effect to average the periodogram over neighboring frequencies. Since then, there has evolved the general concept of smoothing the periodogram with some spectral window $W_T(\omega)$.

The smoothed periodogram is given by the convolution,

$$\hat{P}_T(\omega) = \int_{-\infty}^{\infty} W_T(\omega - \lambda) I_T(\lambda) d\lambda, \quad (3.1)$$

of the raw periodogram with the spectral window.

In the last 20 years, a multitude of smoothing windows have made their appearance. Some of the more popular ones are associated with the names Bartlett, Hamming, Hanning, Parzen, etc. There is still a good deal of controversy over the choice of any specific window to insure an optimal estimate, let alone any initial agreement over a criterion of optimality. This paper does not hope to explore this facet of the problem (the interested reader may consult references 4-9) but only to make the point that, generally, some smoothing is required when the periodogram is used against a random process.

The mechanization of (3.1) for discrete-time data is often quite simple and clearly illustrates Daniell's original suggestion of averaging the periodogram over neighboring values. A particular case being the discrete-time Hanning smoothed periodogram which is given by

$$P_N(\omega_k) = \frac{1}{4} I_N(\omega_{k-1}) + \frac{1}{2} I_N(\omega_k) + \frac{1}{4} I_N(\omega_{k+1}) \quad (3.2)$$

Over the years, this author has found this smoothing algorithm to be as effective as any for run-of-the-mill problems. Its acceptance by this author being its simplicity, especially for implementation on a binary computer.

The smoothed periodogram is also a reasonable choice as an estimator of the spectral density function of noise-free transient waveforms. This is because the smoothing process tends to remove round-off and discretization errors introduced by the computation and yet does not degrade the estimate since the theoretical spectrum is continuous and not subject to sharp jumps or spikes. As an example, Figure 2 presents the smoothed periodogram estimate of the transfer gain characteristic $|H(j\omega)|^2$ derived from the sampled impulse response of the system,

$$H(s) = \frac{\omega_n^2}{s^2 + 2\zeta\omega_n s + \omega_n^2} \quad (3.3)$$

where

$$\omega_n = 6\pi, \quad \zeta = 0.05, \quad \Delta t = 0.005. \quad (3.4)$$

Figure 3 presents the Hanning smoothed periodogram for the complete four-minute seismogram of Figure 1. The earthquake event is indicated by the double spike of energy about 1.0 Hz and by the single spike at 2.0 Hz. The major portion of the energy centered about 0.2 Hz is due to the micro-seismic noise. Additional discussion is postponed until Section IX. Specific details of the program, which were used to determine the estimates of Figures 2 and 3, may be found in reference 10.

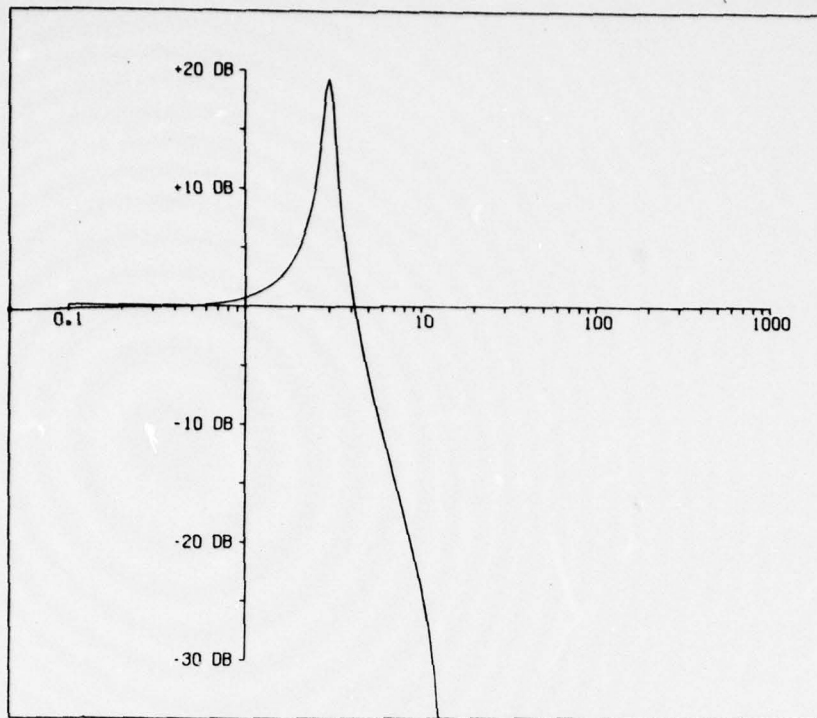


Figure 2 SMOOTHED PERIODOGRAM ESTIMATE OF A TRANSFER GAIN CHARACTERISTIC

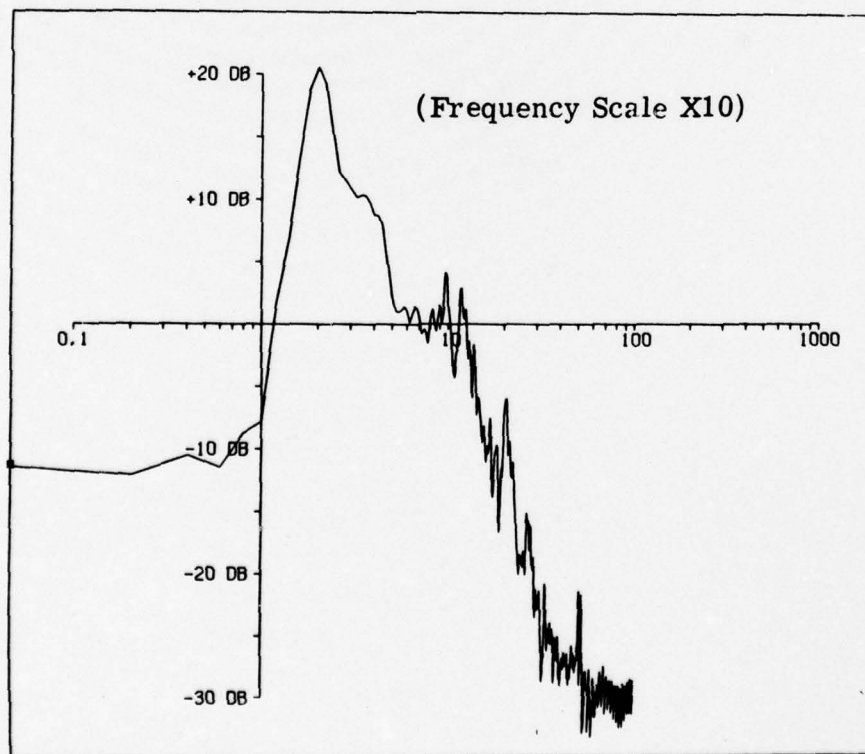


Figure 3 SMOOTHED PERIODOGRAM ESTIMATE OF THE SPECTRUM OF THE SEISMOGRAM

IV. THE FORCED HARMONIC OSCILLATOR

A. The Continuous-Time Case

Consider the forced harmonic oscillator given in state-vector form by

$$\dot{\underline{x}}_k(t) = A_k \underline{x}_k(t) + b u(t) = \begin{bmatrix} 0 & -\omega_k \\ \omega_k & 0 \end{bmatrix} \begin{bmatrix} x_{1k}(t) \\ x_{2k}(t) \end{bmatrix} + \begin{bmatrix} 0 \\ 1 \end{bmatrix} u(t). \quad (4.1)$$

The fundamental matrix for this system is readily found to be

$$\underline{\Phi}_k(t) = e^{A_k t} = \begin{bmatrix} \cos(\omega_k t) & -\sin(\omega_k t) \\ \sin(\omega_k t) & \cos(\omega_k t) \end{bmatrix} \quad (4.2)$$

and the general solution of (4.1) for $\underline{x}_k(0) \equiv 0$ is given by¹¹

$$\underline{x}_k(T) = \int_0^T e^{A_k(T-t)} b u(t) dt = e^{A_k T} \int_0^T \begin{bmatrix} \cos(\omega_k t) & \sin(\omega_k t) & 0 \\ -\sin(\omega_k t) & \cos(\omega_k t) & 1 \end{bmatrix} u(t) dt \quad (4.3)$$

Now consider the norm of the system (4.1) or more specifically, the quantity

$$\frac{1}{T} \left\| \underline{x}_k(T) \right\|^2$$

By inspection of (4.2), one can see that $e^{A_k T}$ is an orthogonal matrix and is thus norm-preserving (i. e., $e^{A_k T}$ is a pure rotation). Hence, from (4.3) one has

$$\frac{1}{T} \left\| \underline{x}_k(T) \right\|^2 = \frac{1}{T} \left\| \begin{bmatrix} \int_0^T u(t) \sin(\omega_k t) dt \\ \int_0^T u(t) \cos(\omega_k t) dt \end{bmatrix} \right\|^2$$

or

$$\frac{1}{T} \left\| \underline{x}_k(T) \right\|^2 = \frac{1}{T} \left\{ \left| \int_0^T u(t) \cos(\omega_k t) dt \right|^2 + \left| \int_0^T u(t) \sin(\omega_k t) dt \right|^2 \right\} \quad (4.4)$$

A comparison of (4.4) with (2.4) now yields a principal result for this paper, namely,

$$\frac{1}{T} \left\| \underline{x}_k(T) \right\|^2 = I_T(\omega_k) \quad (4.5)$$

which shows that the classical periodogram for a discrete set of frequencies can be determined by driving a set of undamped harmonic oscillators (initially quiescent) with the input data sample and then measuring $\frac{1}{T}$ times the square of the norms of the oscillator's state-vector.

B. The Discrete-Time Case

Rather than start from a difference equation, this paper will first derive it from the continuous time case in order to motivate the results of this section plus other results below. Thus, returning to an equivalent form of (4.3) for the continuous-time case, one can write

$$\underline{x}_k(T) = \int_0^T e^{A_k t} \underline{b} u(T-t) dt. \quad (4.6)$$

Now introduce the usual simple minded discrete-time approximation ($t \rightarrow n\Delta t$, $T \rightarrow N\Delta t$, $u(t) \rightarrow u(n)$, etc.),

$$\underline{x}_k(N) = \Delta t \sum_{n=0}^{N-1} B_k^n \underline{b} u(N-n) \quad (4.7a)$$

where

$$B_k = e^{A_k \Delta t} \quad (4.7b)$$

From (4.7a), one can write

$$\begin{aligned} \underline{x}_k(N+1) &= \Delta t \sum_{n=0}^N B_k^n \underline{b} u(N+1-n) \\ &= \Delta t \sum_{n=1}^N B_k^n \underline{b} u(N+1-n) + \Delta t \underline{b} u(N+1) \\ &= \Delta t \sum_{\lambda=0}^{N-1} B_k^{\lambda+1} \underline{b} u(N-\lambda) + \Delta t \underline{b} u(N+1) \\ &= B_k \Delta t \sum_{\lambda=0}^{N-1} B_k^\lambda \underline{b} u(N-\lambda) + \Delta t \underline{b} u(N+1) \end{aligned}$$

$$\underline{x}_k(N+1) = B_k \underline{x}_k(N) + \Delta t \underline{b} u(N+1) \quad (4.8a)$$

Equation (4.8a) which can be written in greater detail as

$$\begin{bmatrix} x_{1k}(N+1) \\ x_{2k}(N+1) \end{bmatrix} = \begin{bmatrix} \cos(\omega_k \Delta t) & -\sin(\omega_k \Delta t) \\ \sin(\omega_k \Delta t) & \cos(\omega_k \Delta t) \end{bmatrix} \begin{bmatrix} x_{1k}(N) \\ x_{2k}(N) \end{bmatrix} + \begin{bmatrix} 0 \\ 1 \end{bmatrix} \Delta t u(N+1) \quad (4.8b)$$

yields an algorithm for discrete filters of a comb filter program.

Now returning to the equivalence of the discrete-time forced harmonic oscillator (4.8) and the discrete-time periodogram, consider again for

$$\omega_k = \frac{2\pi k}{T} = \frac{2\pi k}{N\Delta t},$$

$$B_k = e^{A_k \Delta t} = \begin{bmatrix} \cos\left(\frac{2\pi k}{N}\right) & -\sin\left(\frac{2\pi k}{N}\right) \\ \sin\left(\frac{2\pi k}{N}\right) & \cos\left(\frac{2\pi k}{N}\right) \end{bmatrix}. \quad (4.9)$$

By induction, one can readily show that

$$B_k^n = \begin{bmatrix} \cos\left(\frac{2\pi kn}{N}\right) & -\sin\left(\frac{2\pi kn}{N}\right) \\ \sin\left(\frac{2\pi kn}{N}\right) & \cos\left(\frac{2\pi kn}{N}\right) \end{bmatrix} \quad (4.10)$$

From (4.9) and (4.10), it follows that

$$B_k^{-1} = \tilde{B}_k, \quad B_k^N = I, \quad B_k^{N-n} = B_k^{-n} = B_k^n \quad (4.11)$$

and

$$\tilde{B}_k^n = \begin{bmatrix} \cos\left(\frac{2\pi kn}{N}\right) & \sin\left(\frac{2\pi kn}{N}\right) \\ -\sin\left(\frac{2\pi kn}{N}\right) & \cos\left(\frac{2\pi kn}{N}\right) \end{bmatrix} \quad (4.12)$$

Since (4.7a) can also be written as

$$\underline{x}_n(N) = \Delta t \sum_{n=1}^N B_k^{N-n} \underline{b} u(n) \quad (4.13)$$

$$= \Delta t \sum_{n=1}^N \tilde{B}_k^n \underline{b} u(n)$$

$$\underline{x}_k(N) = \Delta t \sum_{n=1}^N \begin{bmatrix} \sin\left(\frac{2\pi kn}{N}\right) \\ \cos\left(\frac{2\pi kn}{N}\right) \end{bmatrix} u(n) \quad (4.14)$$

one has again the result

$$\begin{aligned} \frac{1}{T} \|\underline{x}_k(N)\|^2 &= \frac{1}{N} \left\{ \left| \sum_{n=1}^N u(n) \sin\left(\frac{2\pi kn}{N}\right) \right|^2 + \left| \sum_{n=1}^N u(n) \cos\left(\frac{2\pi kn}{N}\right) \right|^2 \right\} \\ &= I_N\left(\frac{2\pi k}{N}\right) \end{aligned} \quad (4.15)$$

V. DISCUSSION

At this point let us re-examine the total problem of spectral estimation. This may be summarized by the following chart:

Process	Spectrum	Estimator
Periodic	Discrete	Periodogram
Stochastic	Continuous	Smoothed Periodogram
Transient	Continuous	Smoothed Periodogram

For most real-world problems, however, one does not have isolated processes, but usually a combination, such as periodic and transient waveforms in a noise background. Yet, one is interested in determining a single estimator to work against the combined process. From what has been offered to date, one is reasonably justified in using a smoothed periodogram in all cases, and realizing that discrete spectral lines are spread somewhat by the estimator. The smoothed periodogram is a distinct possibility for the case of interest in this paper, namely for transient in a noise background. So far, this paper has offered three computation techniques for determining the periodogram which may be summarized briefly as:

- T-1. The direct method via (2.2).
- T-2. The correlation method via (2.6) and (2.7).
- T-3. The bank of forced harmonic oscillators given by (4.8) with (4.15).

Some notable difficulties with the periodogram for the problem at hand are, however, summarized as follows:

- D1. The periodogram must be smoothed in order to obtain a continuous spectra for transients and a consistent estimator against noise.
- D2. The periodogram is tied to a fixed time interval hence, both the epoch and duration of any transient must be known.
- D3. The periodogram requires overlapping estimate to be made upon evolutionary processes in order to determine the time-varying spectrum.

The next section presents a variation on technique T-3 above, which meets all the stated objectives to the periodogram and, moreover, the new technique also circumvents a major difficulty of other techniques as offered by Cochran et al,² namely,

- D4. Other techniques require detection and integration with subsequent loss in response time crucial to transient analysis.

VI. THE FORCED DAMPED HARMONIC OSCILLATOR

This section presents the modifications resulting from the introduction of some damping into the harmonic oscillators of Section IV and then goes on to consider how this modification to the technique T-3 yields a very efficient algorithm for spectral estimation free of all the objections raised in the previous section.

In order to add some damping to the formulation for the forced harmonic oscillator of Section IV, one can make the following change in the transition matrix of the system.

$$A_k = \begin{bmatrix} 0 & -\omega_k \\ \omega_k & 0 \end{bmatrix} \longrightarrow A_k = \begin{bmatrix} 0 & -\omega_k \\ \omega_k & -2\zeta\omega_k \end{bmatrix} \quad (6.1)$$

Another choice and the one used by the author is:

$$A_k = \begin{bmatrix} -\alpha & -\omega_0 \\ \omega_0 & -\alpha \end{bmatrix} = \begin{bmatrix} -\zeta\omega_k & -\omega_k\sqrt{1-\zeta^2} \\ \omega_k\sqrt{1-\zeta^2} & -\zeta\omega_k \end{bmatrix} \quad (6.2)$$

For this particular choice, the new fundamental matrix for the k-th filter is readily found to be

$$\Phi_k = e^{A_k t} = \begin{bmatrix} e^{-\alpha t} \cos(\omega_0 t) & -e^{-\alpha t} \sin(\omega_0 t) \\ e^{-\alpha t} \sin(\omega_0 t) & e^{-\alpha t} \cos(\omega_0 t) \end{bmatrix} \quad (6.3)$$

where as usual (ζ is called the damping ratio)

$$\alpha = \zeta\omega_k \quad \text{and} \quad \omega_0 = \omega_k \sqrt{1-\zeta^2} \quad (6.4)$$

The discrete-time algorithm is the same as (4.8a),

$$\underline{x}_k(n+1) = B_k \underline{x}_k(n) + \Delta t \underline{b}_k u(n+1), \quad (6.5)$$

except now the matrix B_k is derived from (6.3) with again

$$B_k = e^{A_k \Delta t} \quad (6.6)$$

As an estimator of the spectral density function, this author proposes that one employ a bank of filters (damped oscillators) covering the frequency range of interest and using the algorithm (6.5). By analogy with the undamped case, the square of the norms of the recursion algorithm's state vector is again taken as a spectral measure (see Figure 4).

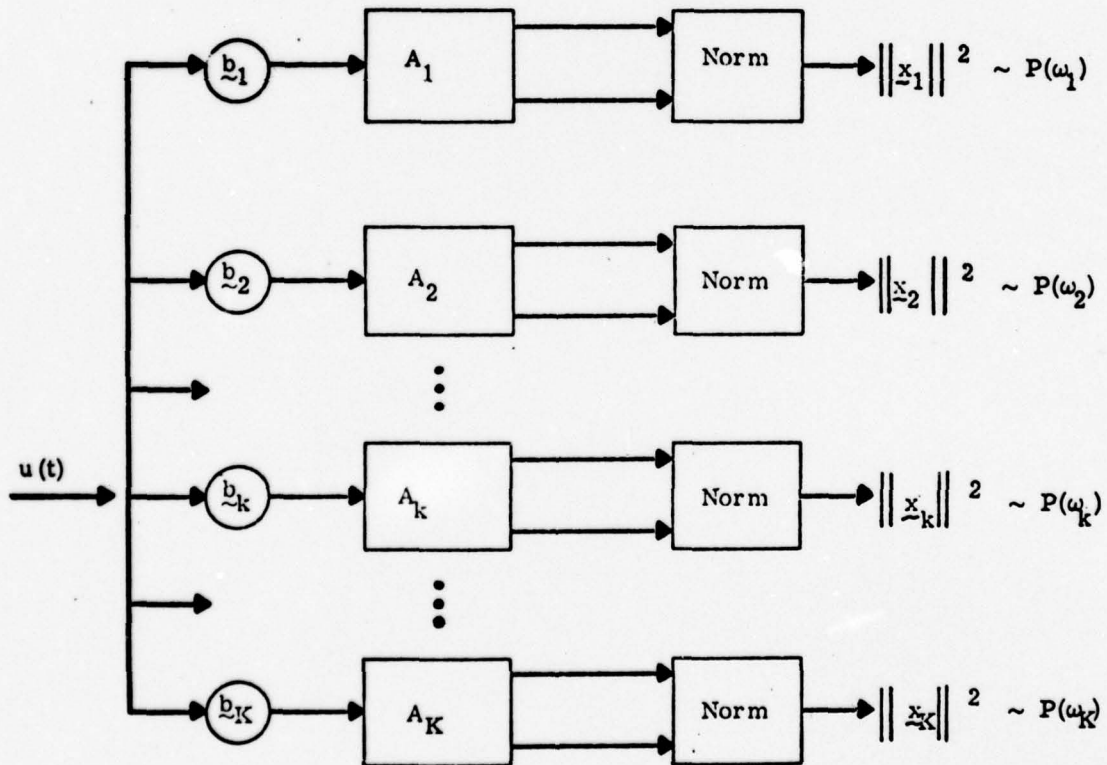


Figure 4 DIGITAL COMB FILTER BANK

Now consider how this proposed estimator meets the objections raised in the previous section. First, as is well known, the introduction of damping detunes the oscillator. This detuning of the harmonic oscillator has the effect that it widens the bandwidth of the system when considered as a bandpass filter. But this is just the desired effect for the smoothing of the periodogram (D1).

Secondly, the filter algorithms can be run "open-loop," since the damping automatically throws away the oldest past input. Moreover, because of its recursive nature, the algorithm is quite efficient numerically. This non-reset capability, coupled with its high numerical efficiency, allows one to start the algorithms well ahead of the initial epoch of any transient. The filter may then be stepped for any desired duration and numerous overlapping spectral estimates may be obtained at will by subsequently calculating the norms of the algorithms state vectors. Hence the second and third objection (D2 and D3) are readily met. Finally, the use of the norms as a spectral measure circumvents the loss of response time due to the usual detection and integration of other techniques (D4).

VII. ADDITIONAL ALGORITHMS FOR THE COMPUTER PROGRAM

A consideration of the input/output transfer functions for the two components of the damped harmonic oscillator's state-vector shows them to be a linear combination of the following:

$$H_1(s) = \frac{\omega_k^2}{s^2 + 2\zeta\omega_k s + \omega_k^2} \quad H_2(s) = \frac{s\omega_k}{s^2 + 2\zeta\omega_k s + \omega_k^2} \quad (7.1)$$

From Figure 2, one can see that the first of these $H_1(s)$ has significant gain at the low end of the spectrum. This response to d-c and other low frequencies by the periodogram is well known and is usually circumvented in other techniques by various mean-removal and detrending operations prior to computation of the periodogram. As an alternative to a detrending operation, the present program differentiates the input time series before application to the various filter algorithms. For discrete-time data, this is nothing more than using the first differences

$$u(n+1) = X_{n+1} - X_n \quad (7.2)$$

to drive the filter algorithms (6.5).

With the introduction of damping into the second order algorithms, one is restricted to a finite bandwidth Δf given by the usual relation¹²

$$Q = \frac{\omega}{\Delta\omega} = \frac{f}{\Delta f} = \frac{1}{2\zeta} \quad (7.3)$$

Also, for many applications, a log frequency scale for the estimated spectrum is desired. This subsequently dictated that the bank of filters be derived on a

basis of constant quality Q . The usual procedure is to overlap the various contiguous filters at their -3dB points as in Figure 5. For any given Q or equivalently for any given damping ratio ζ , the discrete set of center frequencies for the filter bank are readily derived from the algorithm

$$\begin{aligned} f_1 &= (1+\zeta) f_{\text{base}} \\ f_{k+1} &= \left(\frac{1+\zeta}{1-\zeta}\right) f_k \end{aligned} \tag{7.4}$$

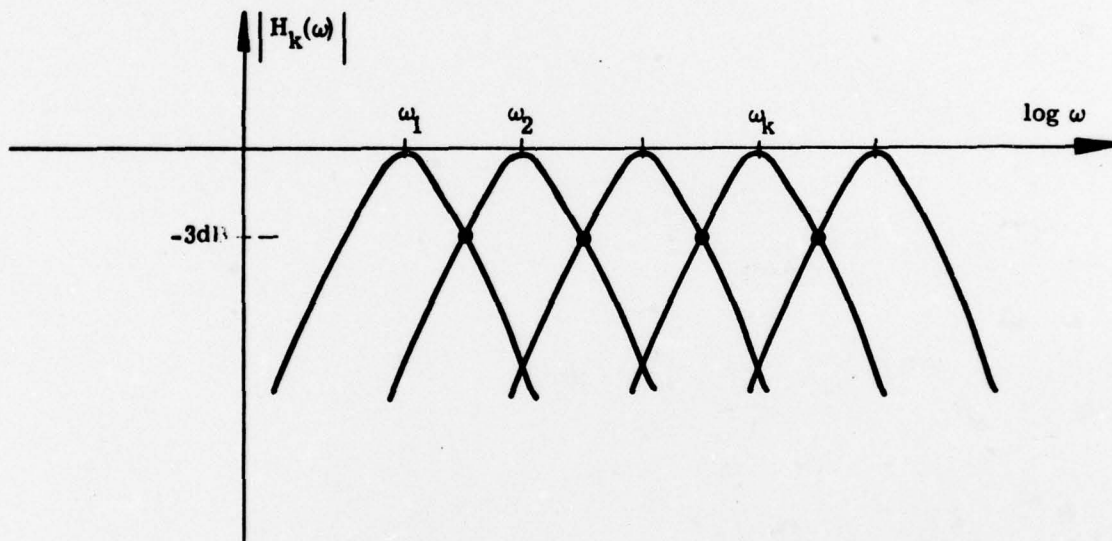


Figure 5 TRANSFER GAIN CHARACTERISTICS OF COMB FILTER BANK

For a damping ratio of $\zeta = 0.115$ and a base frequency of 2.5 Hz, this algorithm produces a program which makes the computer look like a standard 1/3-octave analyzer with the set of center frequencies as given in Table 1.

Table 1

2.79	28.1	283
3.51	35.4	357
4.43	44.6	449
5.58	56.2	566
7.02	70.8	713
8.85	89.2	898
11.15	112.3	1132
14.05	141.5	1426
17.70	178.3	1797
22.30	224.7	2264

Although the proposed estimation scheme does not require any post-detection smoothing, some time smoothing of the state-vector norms has been found beneficial, especially for display purposes. To date, two modes of smoothing have been implemented. The first smoothes (in time) each output vector norm with a low-pass filter whose time constant is fixed, and the same for all frequency bands. The second mode smoothes each output norm by a low-pass filter whose time constant is some fixed proportion of the respective filter's time constant. In either the fixed or proportionally smoothed case, the low-pass filter algorithm is given by

$$\hat{P}_k(n+1) = b_k \hat{P}_k(n) + a_k \left\| \tilde{x}_k(n+1) \right\|^2, \quad (7.5)$$

where in the fixed case,

$$a_k = \alpha_0 \Delta t, \quad b_k = \exp(-\alpha_0 \Delta t); \quad (7.6a)$$

and in the proportional case

$$a_k = \beta 2\pi f_k N_{\Delta t} \Delta t, \quad b_k = \exp(-a_k) \quad (7.6b)$$

for some choice of the parameter β . (The fixed point algorithm of the program requires that $\beta N_{\Delta t} \leq 0.3$.)

VIII. THE COMPUTER PROGRAM

The algorithms proposed in this paper have been implemented upon a Honeywell, Computer Control Division's DDP-24 general purpose computer. The skeleton of the computer program is coded in FORTRAN, but all the plotting and repetitive calculations are coded as machine language subroutines for greater speed and efficiency. Figure 6 presents a flow chart of the complete program. The program is presently configured to accept the input data as records of 500 samples each from magnetic tape. The input control parameters are:

1. NRCD: The number of input data records to be processed.
2. NDT: The plot (and print) increment.
3. DT: The basic time increment Δt of the data.
4. ZETA: The damping ratio ζ .
5. BETA: The output norm smoothing ratio β .

The present program is also configured to cover a three decade scale in frequency from f_{base} to the Nyquist (or folding) frequency f_{Ny} . Since

$$f_{\text{Ny}} = \frac{1}{2\Delta t} \quad , \quad (8.1)$$

the program can thus determine via algorithm (7.4) with

$$f_{\text{base}} = (0.001) f_{\text{Ny}} \quad (8.2)$$

the number of the filters and their proper spacing so as to cover the specified frequency range. With a damping ratio of $\zeta = 0.115$ ($Q \approx 4.3$), one obtains thirty 1/3-octave filter as denoted in Section VII. For $\zeta = 0.03846$, ninety 1/9-octave filters are obtained.

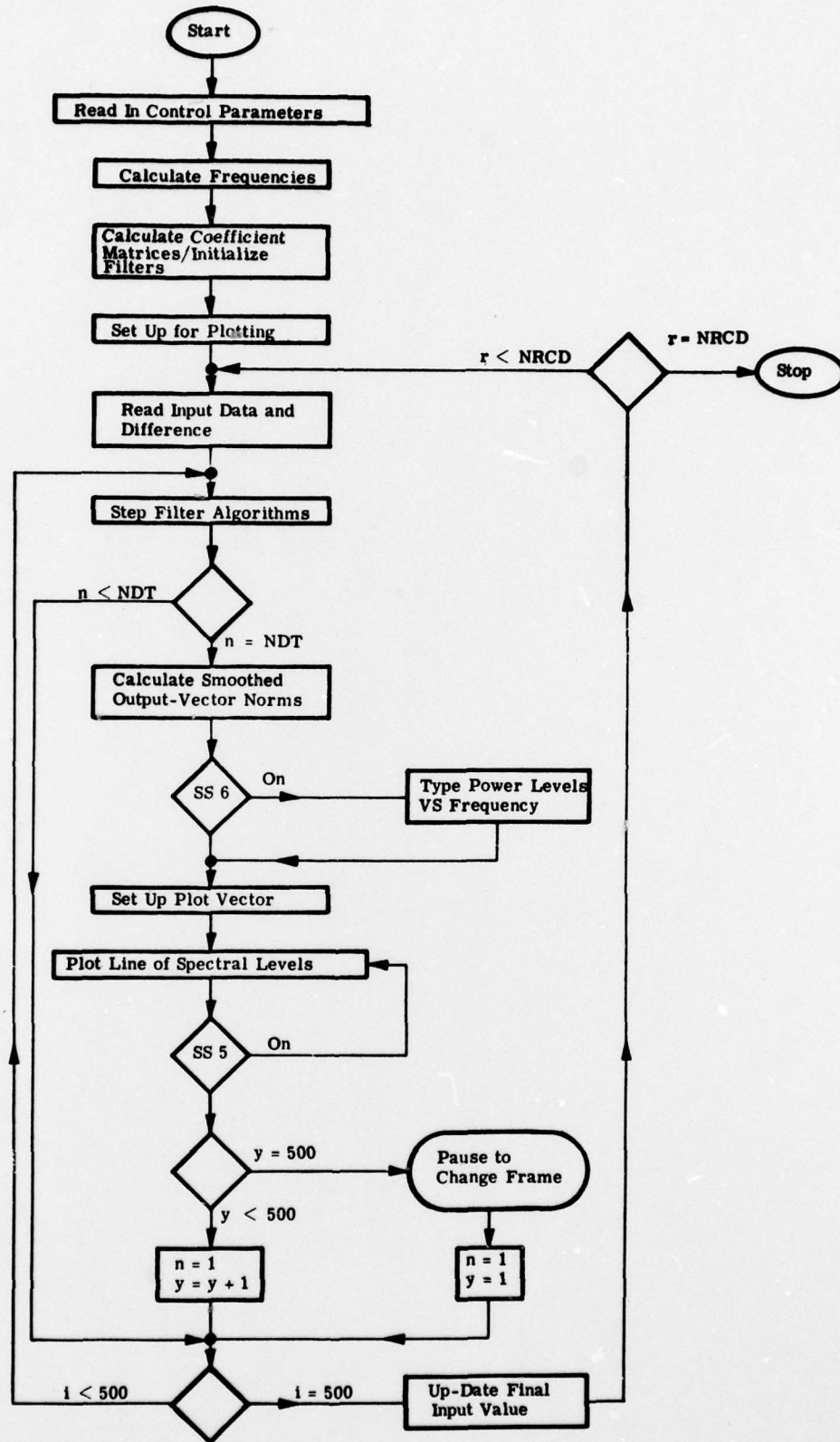


Figure 6 FLOW CHART OF THE COMB FILTER PROGRAM

Except for the mode of output display, the program is quite standard. Fortunately, the Radiation Center has a CRT display with a 512 x 512 x-y resolution interfaced with the DDP-24. In addition, the z-axis or intensity of the display has 16 levels available under program control. With this capability, the computer program is configured to display the evolution of a time-varying spectrum. Starting from the top of the display, each line presents an instantaneous measure of the energy contained in each of the algorithms comprising the filter bank, (increasing frequency left to right). As time evolves (and more data is processed) the horizontal trace is moved down the face of the CRT to provide a time axis to the energy density spectrum (see the figures in the next section). The time scale of the display is controlled by the parameter NDT which is the multiple of the basic sample spacing Δt (DT) used as a display increment; 500 lines comprising one frame. The intensity of the display for any given filter (frequency band) is actually the logarithm (base 2) of the filter's energy and hence each grey scale of the display corresponds to a 3 dB difference in energy.

The entire evolution of the display (and thus the spectrum) is recorded by a camera whose shutter is left open. After one frame has been generated, the computer pauses to allow the operator to remove and reload the camera with a new Polaroid film pack. Restarting the computer provides for continued evolution of the data's spectrum.

IX. SOME RESULTS

The merits of the comb filter technique and the resulting computer program are amply demonstrated by the results presented in this section. The only input data sample considered is the seismogram of Figure 1. The data sample consisted of sampled values (at 20 samples per second) of approximately four minutes of the output of a single seismometer. The estimated 1/9-octave time varying spectrum for the entire data sample by the comb filter program is presented on the left side of Figure 7. On the right side of Figure 7 is an expanded (in time) version of the 1/9 octave spectrum of the central portion of the seismogram which contains an earthquake. Two definite arrivals of the event which spectrally is a double line about 1.0 Hz plus some 2.0 Hz energy can clearly be seen. Also, the after effect has considerable spectral detail. All of the time-varying detail is lost by a conventional periodogram analysis. In fact, if all the energy contained in each frequency band could be projected into one time plane, one would recover the periodogram estimate of the total sample as given in Figure 3.

Figure 8 duplicates the signature on the right in Figure 7 plus presenting an enhanced version obtained by simply restricting the CRT intensity to a cruder quantification. In both Figure 7 and 8, no post-detection (post-norm) smoothing has been applied. It is this minimal response time of the computer program which allows all the time-varying spectral detail to be seen.

Figures 9 and 10 present signatures comparable to those of Figure 7, except in Figure 9, a uniform (across frequency) post-detection smoothing has been applied, and in Figure 10, the post-detection smoothing has been proportional with frequency. In both cases the post-detection

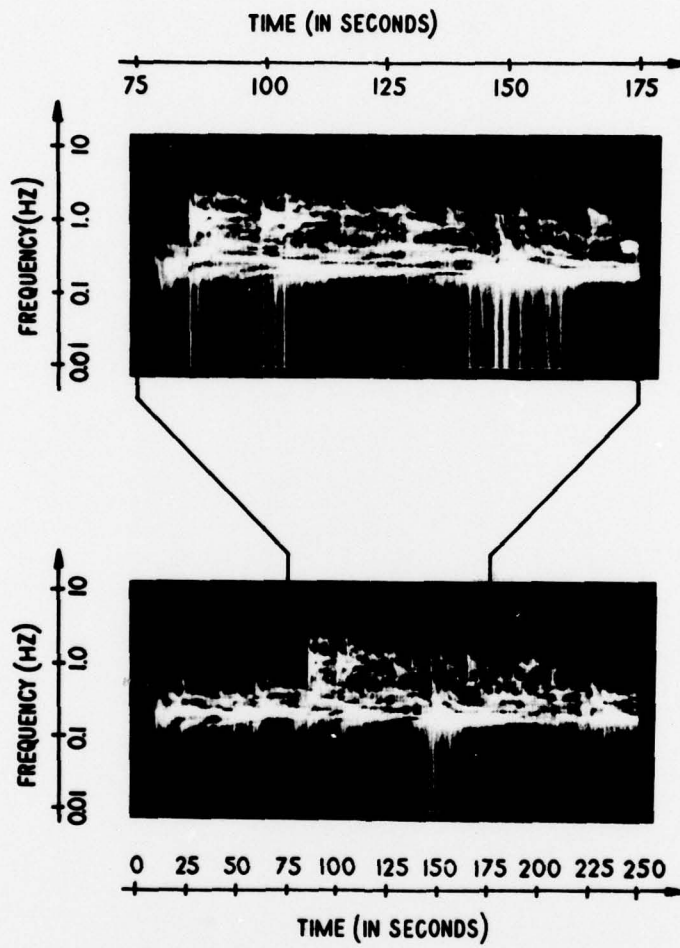
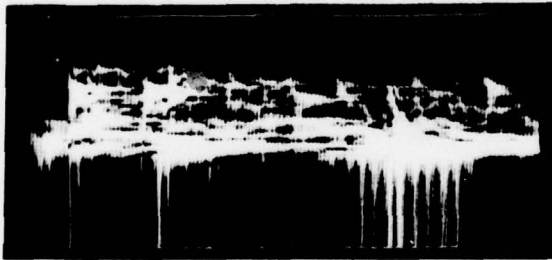


Figure 7 1/9 OCTAVE SIGNATURE OF SEISMIC EVENT (EARTHQUAKE)



4 BIT INTENSITY (16 LEVELS)
3 DB PER GREY SCALE



2 BIT INTENSITY (4 LEVELS)
12 DB PER GREY SCALE

Figure 8 1/9 OCTAVE SIGNATURES OF SEISMIC EVENT

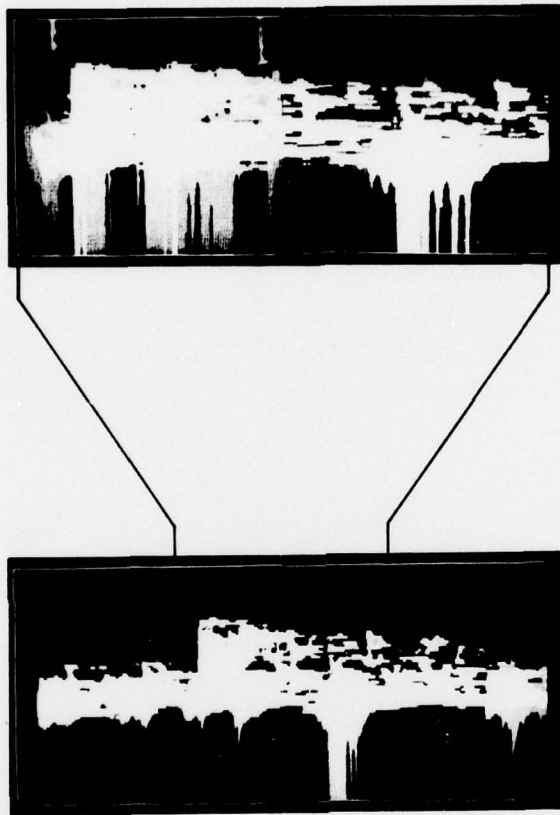
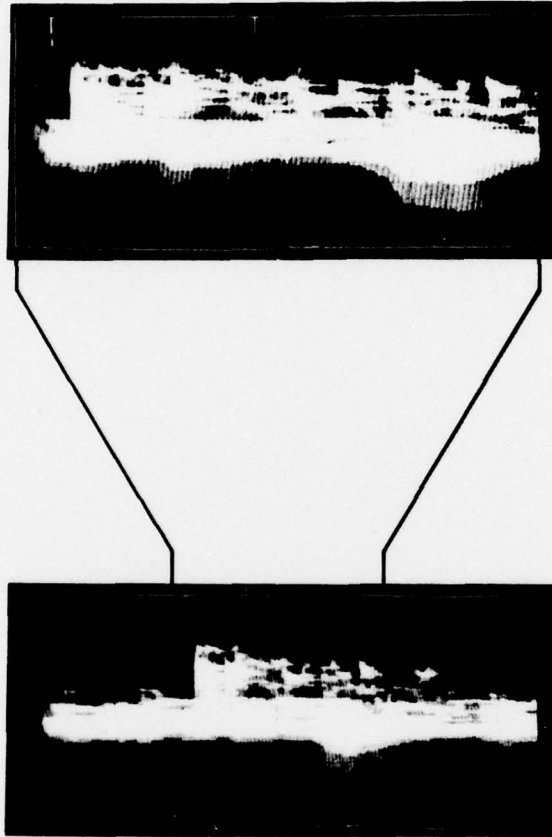


Figure 9 SMOOTHED 1/9 OCTAVE SIGNATURES OF SEISMIC EVENT



$\beta=0.15$ $N_k=2$

$\beta=0.06$ $N_k=5$

Figure 10 SMOOTHED 1/9 OCTAVE SIGNATURES OF SEISMIC EVENT

smoothing tends to degrade the fine time structure of the spectrum. However, for some other applications of the program wherein the transients had narrow band signatures of longer duration, the post-detection smoothing helped to mitigate the effect of the background noise.

X. SUMMARY AND CONCLUSIONS

This paper has offered an alternative technique for the computation of the classical periodogram as the square of the norms of the state-vectors of a set of undamped harmonic oscillators forced by the input data sample. Then after consideration of some of the problems with the periodogram, the paper has shown how the introduction of some damping into the previous formulation produces extremely efficient algorithms for the determination of time-varying spectra.

These algorithms have been implemented into a digital computer program which has subsequently been used to determine the spectral signature of transient waveforms embedded in noise from many areas of application. The high numerical efficiency of the computer program, plus the high degree of detail in the resulting spectra implies that the technique presented in this paper should be considered in any future spectral estimation program.

REFERENCES

1. Swanlund, G. D., The Recognition of Transient Waveforms by Spectral Patterns, Presented at the Spectrum Analysis Techniques Symposium, Honeywell Research Center, Hopkins, Minnesota. (September 1966)
2. Cochran, W. T. et al, Burst Measurements in the Frequency Domain, Proc. IEEE, vol. 54 (June 1966) pp. 830-841.
3. Daniell, P. J., Discussion on Symposium on Autocorrelation in Time-Series, Supplement to the J. Roy. Statist. Soc., vol. 8 (1946) pp. 88-90.
4. Blackman, R. B., and Tukey, J. W., The Measurement of Power Spectra, Dover (1959).
5. Jenkins, G. M., and Priestly, M. B., The Spectral Analysis of Time Series, J. Roy. Statist. Soc., Series B, vol. 19 (1957) pp. 13-37.
6. Jenkins, G. M., General Considerations in the Analysis of Spectra, Technometrics, vol. 3 (1961) pp. 133-166.
7. Parzen, E., Mathematical Considerations in the Estimation of Spectra, Technometrics, vol. 3 (1961) pp. 167-190.
8. Priestley, M. B., Basic Considerations in the Estimation of Spectra, Technometrics, vol. 4 (1962) pp. 551-564.
9. Parzen, E., On Statistical Spectral Analysis, Proc. of a Symposium on Stochastic Processes in Mathematical Physics and Engineering, published by the Amer. Math. Soc. (1964) pp. 221-246.
10. Arnold, C. R., and Korngold, E., A Program for the Estimation of Power Spectra, Lincoln Laboratory Tech. Note 1965-16 (21 May 1965), AD-616 677.
11. Kaplan, W., Operational Methods for Linear Systems, Addison-Wesley (1962) pp. 493-495.
12. Mason, S. J., and Zimmerman, H. J., Electronic Circuits, Signals, and Systems, Wiley (1969) pp. 406-418.